

## Lobophytone H—N, Biscembranoids from the Chinese Soft Coral *Lobophytum pauciflorum*

Pengcheng YAN,<sup>a</sup> Zhiwei DENG,<sup>b</sup> Leen VAN OFWEGEN,<sup>c</sup> Peter PROKSCH,<sup>d</sup> and Wenhan LIN<sup>\*,a</sup>

<sup>a</sup>State Key Laboratory of Natural and Biomimetic Drugs, Peking University; Beijing 100083, P. R. China; <sup>b</sup>Analytical and Testing Center, Beijing Normal University; Beijing, 100875, P. R. China; <sup>c</sup>National Museum of Natural History Naturalis; 2300 RA Leiden, The Netherlands; and <sup>d</sup>Institute of Pharmaceutical Biology and Biotechnology, Heinrich-Heine University; 40225 Duesseldorf, Germany.

Received June 20, 2010; accepted August 31, 2010; published online October 20, 2010

**Chemical examination of a Chinese soft coral *Lobophytum pauciflorum* resulted in the isolation of seven new biscembranoids, named lobophytone H—N (1—7). Their structures were determined by interpretation of 1D- and 2D-NMR (correlation spectroscopy (COSY), heteronuclear single quantum coherence (HSQC), heteronuclear multiple bond connectivity (HMBC), and nuclear Overhauser effect spectroscopy (NOESY)) spectroscopic data in association with MS and IR data. All compounds were tested for the inhibition of lipopolysaccharide (LPS)-induced nitric oxide (NO) production, cytotoxicity of mouse peritoneal macrophage, and antibacterial activities.**

**Key words** soft coral; *Lobophytum pauciflorum*; lobophytone; structure; elucidation

Biscembranoids are a family of marine natural products with unusual structure pattern mainly found from marine soft corals, featured by a 14-6-14 membered tricyclic backbone of tetraterpenoids. Their structures varied mainly in ring C where high oxygenation and tri-, penta-, and hexa-epoxy cyclic moieties are frequently observed. The plausible biogenetic pathway of biscembrane analogues was assumed to be derived by a Diels–Alder cycloaddition of two “mono” cembranoids, representing cembranoid-diene and cembranoid-dienophile.<sup>1–8</sup> This depiction was later supported by the natural occurring monomeric cembranoids, such as dienophiles methyl sarcoate<sup>3</sup> and methyl tetrahydrosarcoate<sup>7</sup> (methyl tortuosoate),<sup>6</sup> which were regarded to be the precursors to form left part of biscembranoids. Biscembranoids were mainly obtained from the coral genus of *Sarcophyton* (*S. tortuosum*, *S. glaucum*, *S. latum*, and *S. elegans*), with the exception of isobiscembranoids<sup>9</sup> recently to be isolated from a soft coral *Lobophytum pauciflorum* which was previously reported to contain steroids<sup>10,11</sup> and diterpenoids.<sup>12–17</sup> As part of our continuing interest in the chemical diversity from soft corals of South China Sea, soft coral *L. pauciflorum* was collected from Sanya Bay, Hainan Island of China. In this paper, we report seven new biscembranoids isolated from the same specimen and their structural elucidation.

### Results and Discussion

Repeated column chromatography including reversed-phase HPLC separation of EtOAc-soluble fraction obtained from the EtOH extract of this specimen yielded seven biscembranoids (1—7) (Fig. 1). All of the isolated biscembranoids shared the partial structure closely related to cembranoid-dienophile methyl tortuosoate.

Lobophytone H (1) had a molecular formula of C<sub>41</sub>H<sub>62</sub>O<sub>8</sub> as determined by high resolution-electrospray ionization-mass spectrum (HR-ESI-MS) (*m/z* 705.4309 [M+Na]<sup>+</sup>, Calcd for C<sub>41</sub>H<sub>62</sub>O<sub>8</sub>Na, 705.4336) and NMR data, requiring 11 degrees of unsaturation. The <sup>1</sup>H-NMR spectrum exhibited proton resonances for nine methyls including three olefinic methyls ( $\delta_{\text{H}}$  1.59, 1.67, 1.71) and a OMe ( $\delta_{\text{H}}$  3.42), while <sup>13</sup>C-NMR spectrum present 41 carbon resonances including three ketones out of four carbonyl resonances, six olefinic carbons, and four oxygen-bearing *sp*<sup>3</sup> carbons (Tables 1, 2). The <sup>1</sup>H- and <sup>13</sup>C-NMR data of 1 featured a structural pattern of biscembranoid. Analysis of 1D- and 2D-NMR spectroscopic data (correlation spectroscopy (COSY), heteronuclear single quantum coherence (HSQC), and heteronuclear multiple bond correlation (HMBC)) in association with IR and MS data defined the gross structure of 1 to be identical to methyl tortuosoate A,<sup>4</sup> a biscembranoid formerly isolated from

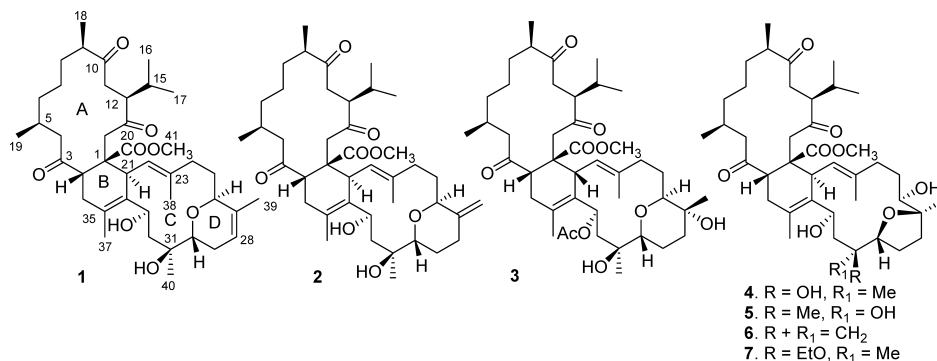


Fig. 1. Structures of Lobophytone H—N (1—7)

\* To whom correspondence should be addressed. e-mail: whlin@bjmu.edu.cn

Table 1.  $^{13}\text{C}$ -NMR Spectroscopic Data of Lobophytone H—N (1—7)<sup>a)</sup>

Position	1	2	3	4	5	6	7
1	48.9 qC	49.1 qC	47.0 qC	49.3 qC	49.3 qC	49.2 qC	49.3 qC
2	44.6 CH	44.5 CH	48.0 CH	43.3 CH	43.6 CH	43.6 CH	43.39 CH
3	213.4 qC	213.7 qC	210.1 qC	213.6 qC	213.6 qC	213.4 qC	213.6 qC
4	52.7 CH <sub>2</sub>	53.1 CH <sub>2</sub>	48.8 CH <sub>2</sub>	53.9 CH <sub>2</sub>	53.8 CH <sub>2</sub>	53.8 CH <sub>2</sub>	53.9 CH <sub>2</sub>
5	27.1 CH	27.1 CH	27.6 CH	27.3 CH	27.3 CH	27.1 CH	27.2 CH
6	37.6 CH <sub>2</sub>	37.7 CH <sub>2</sub>	36.3 CH <sub>2</sub>	37.7 CH <sub>2</sub>	37.7 CH <sub>2</sub>	37.6 CH <sub>2</sub>	37.6 CH <sub>2</sub>
7	25.4 CH <sub>2</sub>	27.1 CH <sub>2</sub>	24.5 CH <sub>2</sub>	25.8 CH <sub>2</sub>	25.8 CH <sub>2</sub>	25.7 CH <sub>2</sub>	25.8 CH <sub>2</sub>
8	34.0 CH <sub>2</sub>	33.8 CH <sub>2</sub>	33.1 CH <sub>2</sub>	33.8 CH <sub>2</sub>	33.9 CH <sub>2</sub>	33.7 CH <sub>2</sub>	33.8 CH <sub>2</sub>
9	47.4 CH	47.6 CH	47.1 CH	47.1 CH	47.2 CH	47.2 CH	47.0 CH
10	213.5 qC	213.3 qC	213.6 qC	213.2 qC	213.3 qC	213.0 qC	213.2 qC
11	33.6 CH <sub>2</sub>	32.3 CH <sub>2</sub>	35.7 CH <sub>2</sub>	31.2 CH <sub>2</sub>	31.1 CH <sub>2</sub>	30.7 CH <sub>2</sub>	31.2 CH <sub>2</sub>
12	51.4 CH	51.3 CH	51.4 CH	52.1 CH	52.0 CH	51.7 CH	52.1 CH
13	211.1 qC	211.0 qC	211.4 qC	209.5 qC	209.7 qC	209.5 qC	209.4 qC
14	46.6 CH <sub>2</sub>	46.6 CH <sub>2</sub>	45.8 CH <sub>2</sub>	45.3 CH <sub>2</sub>	45.5 CH <sub>2</sub>	45.3 CH <sub>2</sub>	45.3 CH <sub>2</sub>
15	29.0 CH	29.0 CH	29.2 CH	28.8 CH	28.6 CH	28.5 CH	28.9 CH
16	21.3 CH <sub>3</sub>	21.3 CH <sub>3</sub>	20.9 CH <sub>3</sub>	21.5 CH <sub>3</sub>	21.2 CH <sub>3</sub>	21.3 CH <sub>3</sub>	21.5 CH <sub>3</sub>
17	18.1 CH <sub>3</sub>	18.0 CH <sub>3</sub>	18.9 CH <sub>3</sub>	17.9 CH <sub>3</sub>	17.6 CH <sub>3</sub>	17.3 CH <sub>3</sub>	17.6 CH <sub>3</sub>
18	17.4 CH <sub>3</sub>	17.5 CH <sub>3</sub>	17.1 CH <sub>3</sub>	17.6 CH <sub>3</sub>	17.6 CH <sub>3</sub>	17.4 CH <sub>3</sub>	17.6 CH <sub>3</sub>
19	22.6 CH <sub>3</sub>	22.7 CH <sub>3</sub>	22.0 CH <sub>3</sub>	22.7 CH <sub>3</sub>	22.8 CH <sub>3</sub>	22.6 CH <sub>3</sub>	22.7 CH <sub>3</sub>
20	174.5 qC	174.7 qC	175.4 qC	174.7 qC	174.9 qC	174.5 qC	174.7 qC
21	42.1 CH	42.1 CH	45.5 CH	43.4 CH	43.6 CH	43.4 CH	43.4 CH
22	123.5 CH	123.5 CH	124.4 CH	126.9 CH	127.2 CH	127.0 CH	127.0 CH
23	136.2 qC	135.6 qC	138.2 qC	137.4 qC	136.6 qC	136.7 qC	137.3 qC
24	35.8 CH <sub>2</sub>	35.8 CH <sub>2</sub>	39.2 CH <sub>2</sub>	37.1 CH <sub>2</sub>	36.6 CH <sub>2</sub>	36.2 CH <sub>2</sub>	36.9 CH <sub>2</sub>
25	29.7 CH <sub>2</sub>	30.9 CH <sub>2</sub>	23.4 CH <sub>2</sub>	28.7 CH <sub>2</sub>	28.0 CH <sub>2</sub>	28.0 CH <sub>2</sub>	28.6 CH <sub>2</sub>
26	78.4 CH	80.5 CH	83.2 CH	72.6 CH	71.8 CH	72.0 CH	72.2 CH
27	134.9 qC	149.2 qC	68.6 qC	85.8 qC	85.9 qC	85.7 qC	86.1 qC
28	120.1 CH	28.8 CH <sub>2</sub>	33.1 CH <sub>2</sub>	35.5 CH <sub>2</sub>	35.5 CH <sub>2</sub>	35.6 CH <sub>2</sub>	35.0 CH <sub>2</sub>
29	25.4 CH <sub>2</sub>	25.6 CH <sub>2</sub>	20.4 CH <sub>2</sub>	27.7 CH <sub>2</sub>	26.3 CH <sub>2</sub>	30.5 CH <sub>2</sub>	28.4 CH <sub>2</sub>
30	68.4 CH	71.9 CH	71.2 CH	87.9 CH	89.2 CH	84.7 CH	83.9 CH
31	72.9 qC	72.7 qC	73.6 qC	74.7 qC	72.0 qC	149.3 qC	79.9 qC
32	43.0 CH <sub>2</sub>	42.4 CH <sub>2</sub>	41.0 CH <sub>2</sub>	39.1 CH <sub>2</sub>	42.0 CH <sub>2</sub>	35.1 CH <sub>2</sub>	38.6 CH <sub>2</sub>
33	66.0 CH	65.5 CH	73.5 CH	66.8 CH	64.7 CH	67.6 CH	66.0 CH
34	132.9 qC	133.0 qC	131.8 qC	133.4 qC	135.6 qC	134.0 qC	133.7 qC
35	126.0 qC	126.5 qC	126.4 qC	123.9 qC	122.2 qC	124.5 qC	123.8 qC
36	33.1 CH <sub>2</sub>	33.0 CH <sub>2</sub>	32.7 CH <sub>2</sub>	32.8 CH <sub>2</sub>	32.7 CH <sub>2</sub>	32.5 CH <sub>2</sub>	32.8 CH <sub>2</sub>
37	19.2 CH <sub>3</sub>	19.2 CH <sub>3</sub>	20.5 CH <sub>3</sub>	17.6 CH <sub>3</sub>	18.1 CH <sub>3</sub>	18.0 CH <sub>3</sub>	18.0 CH <sub>3</sub>
38	19.6 CH <sub>3</sub>	19.7 CH <sub>3</sub>	15.9 CH <sub>3</sub>	16.6 CH <sub>3</sub>	16.7 CH <sub>3</sub>	16.4 CH <sub>3</sub>	16.6 CH <sub>3</sub>
39	20.5 CH <sub>3</sub>	107.4 CH <sub>2</sub>	26.7 CH <sub>3</sub>	21.4 CH <sub>3</sub>	21.5 CH <sub>3</sub>	20.8 CH <sub>3</sub>	21.5 CH <sub>3</sub>
40	25.1 CH <sub>3</sub>	25.4 CH <sub>3</sub>	25.8 CH <sub>3</sub>	23.6 CH <sub>3</sub>	28.4 CH <sub>3</sub>	109.8 CH <sub>2</sub>	20.1 CH <sub>3</sub>
OMe	51.3 CH <sub>3</sub>	51.3 CH <sub>3</sub>	52.0 CH <sub>3</sub>	51.1 CH <sub>3</sub>	51.0 CH <sub>3</sub>	51.0 CH <sub>3</sub>	51.2 CH <sub>3</sub>
EtO							56.9 CH <sub>2</sub>
							16.52 CH <sub>3</sub>
Ac			169.9 qC				
			21.5 CH <sub>3</sub>				

a) Spectra were measured in DMSO-*d*<sub>6</sub>.

*S. tortuosum*. The noticeable difference was found by *J* values of H-33 ( $\delta_{\text{H}}$  4.83, dd,  $J=4.5, 8.0$  Hz) and chemical shift of C-33 ( $\delta_{\text{C}}$  66.0) in **1** to replace the corresponding proton ( $\delta_{\text{H}}$  4.81, br d,  $J=9.5$  Hz) and carbon ( $\delta_{\text{C}}$  70.1, s) of the latter compound. These findings suggested the chiral configuration of C-33 in **1** to be in opposite to that of methyl tortuoate A. The nuclear Overhauser effect (NOE) correlations of H-33/H<sub>3</sub>-37 ( $\delta_{\text{H}}$  1.71), H-33/OH-31 ( $\delta_{\text{H}}$  4.54, s), and H-33/H-22 ( $\delta_{\text{H}}$  4.91, d,  $J=9.5$  Hz), and the absence of NOE correlation between H-33/H-21 as observed in methyl tortuoate A, suggested H-33 being  $\beta$ -oriented. Thus, **1** is a C-33 epimer of methyl tortuoate A. In addition, the NOE correlations and the *J* values of the protons locating at rings C and D were close similar to those of lobophytone A,<sup>9)</sup> whose absolute configurations were determined by X-ray diffraction. Since lobophytone A was isolated from the same specimen as **1**, the configurations in rings C and D of **1** were biogenetically assumed to be the same as those of lobophytone A.

Spectroscopic analysis and comparison of NMR and MS data revealed that the gross structure of lobophytone **1** (**2**) was identical to ximaolide E,<sup>6)</sup> a biscembrane originated from *S. tortuosum*. However, nuclear Overhauser enhancement spectroscopy (NOESY) relationships between H-33/H<sub>3</sub>-37 ( $\delta_{\text{H}}$  1.71, s) and H-33/H-30 ( $\delta_{\text{H}}$  3.38, m) and absence of NOE correlation between H-33/H-21 as observed in ximaolide E, indicated that H-33 ( $\delta_{\text{H}}$  4.83, dd,  $J=3.0, 9.0$  Hz) of **2** was  $\beta$ -oriented as the case of **1**. The similar NOE relationships of **2** in comparison with that of **1** indicated that **2** maintained the same configurations in respect to rings C and D of **1**. Biogenetically, the structure of **2** was considered to be derived from **1** through an olefin conversion from C-27/C-28 to C-27/C-39. Thus, lobophytone **1** (**2**) was determined to be a C-33 epimer of ximaolide E.

The molecular formula of lobophytone **J** (**3**) was determined to be C<sub>43</sub>H<sub>66</sub>O<sub>10</sub> on the basis of HR-ESI-MS data ( $m/z$  765.4540 [M+Na]<sup>+</sup>). Analysis of 1D- and 2D-NMR spectro-

Table 2.  $^1\text{H-NMR}$  Spectroscopic Data of Lobophytones H—N (1—7)<sup>a)</sup>

Position	1	2	3	4	5	6	7
2	3.65 dd (6.1, 8.3)	3.68 dd (6.4, 9.0)	3.40 m	3.40 m	3.39 m	3.46 t (8.6)	3.40 t (8.4)
4	2.88 dd (9.5, 19.3)	2.93 dd (9.8, 19.8)	3.14 m	3.17 dd (10.3, 19.6)	3.16 dd (10.3, 19.6)	3.15 dd (10.3, 19.6)	3.17 dd (10.5, 19.3)
	2.40 d (19.3)	2.42 dd (2.2, 19.8)	2.34 m	2.40 d (20.0)	2.43 d (19.6)	2.44 d (19.6)	2.45 dd (2.9, 19.3)
5	1.74 m	1.73 m	1.86 m	1.73 m	1.68 m	1.67 m	1.69 m
6	1.03 m	1.02 m	1.15 m	1.02 m	1.01 m	1.01 m	1.00 m
	0.89 m	0.95 m	0.90 m	1.05 m	1.08 m	1.06 m	1.05 m
7	0.98 m	1.73 m	0.89 m	1.13 m	1.15 m	1.15 m	1.20 m
	0.90 m	1.74 m	0.92 m	1.02 m	1.01 m	1.00 m	1.00 m
8	1.40 m	1.40 m	1.53 m	1.45 m	1.48 m	1.44 m	1.50 m
	1.50 m	1.44 m	1.42 m	1.35 m	1.35 m	1.35 m	1.38 m
9	2.30 m	2.30 m	2.28 m	2.40 m	2.38 m	2.35 m	2.40 m
11	2.80 dd (10.0, 17.4)	2.82 dd (10.8, 16.9)	2.77 m	2.75 dd (10.3, 16.9)	2.80 m	2.80 m	2.77 dd (10.3, 16.6)
	1.98 d (17.4)	1.94 d (16.9)	2.27 m	1.87 d (16.9)	1.86 m	1.85 m	1.88 d (16.6)
12	2.87 m	2.88 m	2.75 m	2.91 m	2.90 m	2.90 m	2.90 m
14	3.01 d (19.8)	3.02 d (19.8)	2.95 d (19.3)	2.82 d (18.6)	2.81 d (19.0)	2.83 s	2.83 d (19.1)
	2.78 d (19.8)	2.76 d (19.8)	2.87 d (19.3)	2.72 d (18.6)	2.78 d (19.0)	2.80 s	2.66 d (19.1)
15	2.14 m	2.20 m	1.98 m	2.29 m	2.37 m	2.35 m	2.26 m
16	0.92 d (6.9)	0.92 d (6.9)	0.87 d (6.9)	0.97 d (6.6)	0.97 d (6.8)	0.97 d (6.9)	0.96 d (6.6)
17	0.67 d (6.9)	0.65 d (6.9)	0.75 d (6.9)	0.64 d (6.6)	0.63 d (6.8)	0.64 d (6.9)	0.63 d (6.6)
18	1.06 d (6.9)	1.06 d (6.9)	1.09 d (6.9)	1.05 d (6.9)	1.05 d (6.9)	1.06 d (6.9)	1.05 d (6.6)
19	0.81 br s	0.82 d (6.9)	0.86 d (6.9)	0.82 d (6.9)	0.82 d (6.9)	0.82 d (6.9)	0.82 d (6.9)
21	3.47 d (11.0)	3.45 d (11.0)	3.59 d (11.0)	3.54 d (10.5)	3.54 d (10.5)	3.39 d (10.5)	3.58 d (10.5)
22	4.91 d (11.0)	5.01 d (11.0)	5.16 d (11.0)	4.82 d (10.5)	4.80 d (10.5)	4.86 d (10.5)	4.82 d (10.5)
24	2.27 m	2.32 m	2.42 m	1.99 m	1.95 m	1.98 m	1.98 m
	1.74 m	1.74 m	2.04 m	2.03 m	2.02 m	2.00 m	2.01 m
25	1.70 m	2.19 m	1.73 m	1.73 m	1.58 m	1.63 m	1.71 m
		1.25 m	1.54 m	1.20 m	1.15 m	1.19 m	1.20 m
26	3.85 d (6.0)	4.08 d (11.2)	3.38 m	2.99 d (9.1)	2.96 br d (9.3)	3.06 dd (6.3, 9.3)	2.97 dd (5.6, 8.3)
28	5.46 br t (3.0)	2.20 m	1.53 m	2.20 m	2.25 m	2.25 m	2.22 m
		2.22 m	1.42 m	1.40 m	1.35 m	1.45 m	1.37 m
29	1.95 m	1.26 m	1.74 m	1.73 m	1.65 m	1.75 m	1.68 m
	1.76 m	1.50 m	1.40 m	1.41 m	1.56 m	1.55 m	1.38 m
30	3.33 m	3.38 m*	3.30 dd (3.8, 10.3)	3.79 dd (6.8, 8.7)	3.68 dd (6.3, 10.0)	4.36 dd (5.9, 9.7)	4.09 dd (6.1, 9.8)
32	1.88 dd (8.0, 13.9)	1.86 dd (9.0, 13.7)	1.93 m	2.06 dd (11.5, 14.4)	1.50 m	2.10 m	2.27 dd (10.5, 15.2)
	1.31 dd (4.5, 13.9)	1.25 dd (3.0, 13.7)	1.84 m	0.88 d (14.4)	1.06 m	1.90 m	0.90 d (15.2)
33	4.83 dd (4.5, 8.0)	4.83 dd (3.0, 9.0)	4.85 d (11.2)	4.88 d (11.5)	4.86 d (10.0)	4.63 dd (3.9, 9.0)	4.82 d (10.5)
36	2.29 dd (8.3, 19.0)	2.31 dd (9.8, 19.1)	2.48 m	2.30 m	2.25 m	2.27 m	2.25 m
	2.04 dd (6.1, 19.0)	2.06 dd (6.4, 19.1)	1.88 m	1.98 m	1.93 m	2.04 m	1.98 m
37	1.71 s	1.71 s	1.72 s	1.59 s	1.60 s	1.61 s	1.59 s
38	1.67 s	1.63 s	1.75 s	1.61 s	1.58 s	1.54 s	1.61 s
39	1.59 s	4.69 s	1.01 s	1.01 s	0.98 s	1.01 s	1.02 s
		4.63 s					
40	0.94 s	0.93 s	1.06 s	1.03 s	1.21 s	5.00 br s	1.08 s
						4.92 br s	
OMe	3.42 s	3.41 s	3.48 s	3.40 s	3.40 s	3.41 s	3.40 s
EtO							3.50 dq (7.0, 12.0)
							3.45 dq (7.0, 12.0)
							1.04 t (7.0)
Ac			1.88 s				

a) Spectra were measured in DMSO-*d*<sub>6</sub>. \* Overlapped with H<sub>2</sub>O signal.

scopic data revealed that the gross structure of **3** was closely related to that of nyalolide,<sup>7)</sup> a biscembrane analogue also isolated from the same specimen.<sup>9)</sup> The presence of an acetyl group was observed from the NMR spectra at  $\delta_{\text{H}}$  1.88 (3H, s) in addition to  $\delta_{\text{C}}$  21.5 (q) and 169.9 (s). The HMBC relationships from H-33 ( $\delta_{\text{H}}$  4.85, d,  $J=11.2$  Hz) to C-34 and C-35 revealed an oxymethine to be located at C-33 of **3** rather than at C-31 of nyalolide. Additional HMBC correlation between H-33 ( $\delta_{\text{H}}$  4.85, d,  $J=11.2$  Hz) and acetyl carbonyl carbon ( $\delta$  169.9) ascertained the acetoxy group to be substituted at C-33. The relative configurations of **3** were determined by coupling constants and NOE data in association with its NMR data comparing to known compounds. The NOE interaction between H-21 ( $\delta_{\text{H}}$  3.59, d,  $J=11.0$  Hz) and H<sub>3</sub>-38 ( $\delta_{\text{H}}$  1.75, s)

was indicative of 22*E* geometry. The NOESY cross-peaks from H-26 ( $\delta_{\text{H}}$  3.38, dd) to H<sub>3</sub>-40 ( $\delta_{\text{H}}$  1.06, s) and H-24a ( $\delta_{\text{H}}$  2.04, m) and between H-22 ( $\delta_{\text{H}}$  5.16, d,  $J=11.0$  Hz) and H-24a assigned to the same face of H-26, H<sub>3</sub>-40, and H-22, which were in opposite to that of H<sub>3</sub>-38. Additional NOE interactions between H-30 ( $\delta_{\text{H}}$  3.30, dd,  $J=3.8, 10.3$  Hz)/H-33, H-30/H-28a ( $\delta_{\text{H}}$  1.53, m), and H<sub>3</sub>-39 ( $\delta_{\text{H}}$  1.01, s)/H-28a suggested the same orientation of H-30, H-33, and H<sub>3</sub>-39. Moreover, the strong NOE cross-peaks between H-21/H<sub>3</sub>-38, H-21/H-33, and H-33/H<sub>3</sub>-38 indicated the same face of H-21 and H-33. It is noted that all known biscembranoids exclusively showed  $\beta$ -orientation of MeO group, while  $\alpha$ -oriented H-21 resulted in NOE relationship between MeO and H-22. In compound **3**, the presence of NOE relationship between

MeO/H-21 but absence of MeO/H-22 relationship suggested  $\beta$ -face of H-21. Thus, the relative configurations of **3** were determined to be the same as those of lobophytone B,<sup>9)</sup> in which  $\beta$ -orientations of H-21, H-30, H-33, and H<sub>3</sub>-39 and  $\alpha$ -orientations of H-26 and H<sub>3</sub>-40 were assigned.

The graphic structure of **3** was almost identical to ximaolides F<sup>18)</sup> except for the different orientation of AcO at C-33. However, comparison of NMR data revealed downfield shifted C-26 ( $\delta_C$  83.2) and upfield shifted C-27 ( $\delta_C$  68.6) and C-30 ( $\delta_C$  71.2) of **3** to replace those ( $\delta_C$  73.8, 83.6, 88.9, respectively) of ximaolide F. These findings suggested ximaolides F (also G<sup>18)</sup>) containing an ether bridge across C-27 and C-30 as in the case of bisglaucumliides G and H<sup>8)</sup> rather than the ether bridge between C-26/C-30 as reported in literature.

The 1D- and 2D-NMR spectroscopic analysis in association with HR-ESI-MS data resulted in the gross structure of lobophytone K (**4**) to be close similar to that of ximaolide C,<sup>6)</sup> except for the presence of an additional hydroxy group and the absence of a chlorine atom. The replacement of a hydroxy group of **4** to a chlorine atom at C-31 of ximaolide C was evident from OH-31 resonance ( $\delta_H$  4.10, s) and its HMBC correlations to C-32 ( $\delta_C$  39.1), C-31 ( $\delta_C$  74.7), and C-30 ( $\delta_C$  87.9). The relative configurations of rings A and B in **4** were in agreement with those of ximaolide C based on the similar NMR data and NOE relationships. However, the NOE correlations of H-22 ( $\delta_H$  4.82, d,  $J=10.5$  Hz)/H-2 ( $\delta_H$  3.40) and H-22/H-26 ( $\delta_H$  2.99, d,  $J=9.1$  Hz) were assignable to H-26 $\beta$  (Fig. 2). Additional NOE cross-peaks between H-30 ( $\delta_H$  3.79, dd,  $J=6.8, 8.7$  Hz)/H<sub>3</sub>-40 and H-30/H<sub>3</sub>-39 ( $\delta_H$  1.01) determined H-30, H<sub>3</sub>-39, and H<sub>3</sub>-40 to be  $\alpha$ -oriented, while the NOE relationships between H-33 ( $\delta_H$  4.88, d,  $J=11.5$  Hz)/H<sub>3</sub>-40 ( $\delta_H$  1.03) and H-33/H<sub>3</sub>-37 suggested  $\beta$ -face of H-33.

Lobophytone L (**5**) had the same molecular formula as **4**, as determined by HR-ESI-MS and NMR data. The <sup>1</sup>H- and <sup>13</sup>C-NMR data (Tables 1, 2) of **5** and **4** were almost identical, indicating **5** to be a stereoisomer of **4**. The difference was found by the obvious downfield shifted H<sub>3</sub>-40 ( $\delta_H$  1.21) and C-40 ( $\delta_C$  28.4) of **5** in comparison with the corresponding signals of **4** ( $\delta_H$  1.03,  $\delta_C$  23.6). These findings implied that **5** was an epimer of **4** with respect to C-31. The NOE cross-peaks between H<sub>3</sub>-40/H-29 and OH-31/H-33, along with the similar NOE correlations of the remaining protons of both compounds confirmed H<sub>3</sub>-40 to be  $\beta$ -oriented.

HR-ESI-MS and NMR spectroscopic analysis revealed that the structure of lobophytone M (**6**) was closely related to that of **4**. The only difference was found by the presence of an *exo*-methylene group whose <sup>1</sup>H-NMR exhibited at  $\delta$  5.00 (1H, br s) and 4.92 (1H, br s), while the corresponding carbon resonances were assigned to  $\delta$  109.8 (CH<sub>2</sub>) and 149.3 (qC). The position of this group was located at C-31 based on the HMBC correlations from the *exo*-methylene protons to C-30 ( $\delta$  84.7) and C-32. The relative configurations of the chiral centers in rings C and D of **6** were the same as **4** as evident from the similar NMR and NOE data.

The IR and 1D- and 2D-NMR spectroscopic data (Tables 1, 2) of lobophytone N (**7**) revealed that it is a C-31 ethoxy-lated derivative of **4**, as evident from the ethoxy resonances for a methyl at  $\delta_H$  1.04 (3H, t,  $J=7.0$  Hz) and  $\delta_C$  16.5 (CH<sub>3</sub>), and the oxymethylene at  $\delta_H$  3.50 (1H, q,  $J=7.0$  Hz, H-42a)

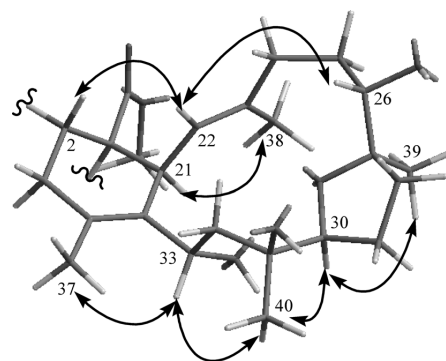


Fig. 2. Key NOE Correlations of **4** Related to Rings C and D

Table 3. Inhibition of LPS-Induced NO Production and Cytotoxicity against PEM $\Phi$ <sup>a)</sup>

Compounds	Concentration ( $\mu$ M)	Level of NO ( $\mu$ M)	IR (%)
DMSO		1.21	
LPS		25.13	
Dex	1.0	1.26	95.00
<b>1</b>	1.0	15.85	22.84
<b>2</b>	1.0	20.12	19.96
<b>3</b>	1.0	18.84	25.04
<b>4</b>	1.0	22.90	8.89
<b>5</b>	1.0	15.75	23.35
<b>6</b>	1.0	23.14	7.93
<b>7</b>	1.0	20.46	18.58

a) PEM $\Phi$ =mouse peritoneal macrophage; IR=inhibition rate against PEM $\Phi$ ; LPS=lipopolysaccharide; Dex=dexamethasone.

and 3.45 (1H, q,  $J=7.0$  Hz, H-42b) and the corresponding <sup>13</sup>C resonance at  $\delta_C$  56.9 (CH<sub>2</sub>), in association with the HMBC correlation from oxymethylene to the downfield shifted C-31 ( $\delta_C$  79.9). The similar NMR and NOE data indicated that **7** shared the same relative configurations of **4**.

In primary assay, all compounds showed weak effect to inhibit lipopolysaccharide (LPS)-induced nitric oxide (NO) production and cytotoxicity against mouse peritoneal macrophage (PEM $\Phi$ ) (Table 3), and possessed weakly inhibitory activity against *Pseudomonas aeruginosa*, *Escherichia coli*, *Candida albicans*, *Aspergillus fumigatus*, *A. flavus*, and *Fusarium oxysporum*.

#### Experimental

**General Experimental Procedures** Optical rotations were measured on a Perkin-Elmer 243B polarimeter. IR spectra were determined on a Thermo Nicolet Nexus 470 Fourier transform (FT)IR spectrometer. <sup>1</sup>H- and <sup>13</sup>C-NMR and 2D-NMR spectra were recorded on an Avance-500 FT 500 MHz NMR spectrometer (Bruker) using tetramethyl silane (TMS) as an internal standard. Chemical shifts ( $\delta$ ) are expressed in parts per million (ppm), and coupling constants ( $J$ ) are reported in Hertz (Hz). HR-ESI-MS spectra were obtained from the Bruker APEX IV instruments. Column chromatography was carried out with Si gel (160–200 mesh and 200–300 mesh), while GF<sub>254</sub> Si gel for TLC was provided by Qingdao Marine Chemistry Co., Ltd. HPLC chromatography was performed on an Alltech instrument (426-HPLC pump, Alltech UV-vis-200 detector) equipped with Kromasil semipreparative (10  $\mu$ m, ODS, 10 mm $\times$ 250 mm) and YMC-Pack C<sub>8</sub> (5  $\mu$ m, 10 mm $\times$ 250 mm) columns.

**Animal Material** Soft coral *Lobophytum pauciflorum* was collected from the inner coral reef at a depth of 10 m in Sanya Bay, Hainan Island of China, in 2008. The fresh samples (2.3 kg, wet weight) were frozen immediately. The specimen was identified by Leen van Ofwegen (National Museum of Natural History Naturalis). The coral specimen (HSF-6) was deposited

at the State Key Laboratory of Natural and Biomimetic Drugs, Peking University, P.R. China.

**Extraction and Isolation** The frozen soft coral *L. pauciflorum* was homogenized and then extracted with EtOH. The concentrated extract was desalted by dissolving in MeOH to yield a residue (92.7 g). This residue was partitioned between H<sub>2</sub>O and EtOAc, and then *n*-BuOH. The EtOAc fraction (12.1 g) was subjected to Si gel column chromatography eluting with a gradient (petroleum ether–acetone, 20 : 1, 10 : 1, 3 : 1, 1 : 1) to obtain seven fractions (F1–F7). F1–F4 mainly contained lipids and steroids, as detected by <sup>1</sup>H-NMR, while F5 and F6 showed the spectral features of biscembranes. Thus, F5 and F6 were combined (1.69 g) and subsequently subjected to Sephadex LH-20 eluting with CH<sub>2</sub>Cl<sub>2</sub>–MeOH (1 : 2) to afford 6 subfractions (SF1–SF6). SF2 (180 mg) showed blue-green spots after spraying with anisaldehyde, and was then separated on reversed-phase semipreparative HPLC with CH<sub>3</sub>CN–H<sub>2</sub>O (61%) as a mobile phase to obtain **5** (2.8 mg). SF3 (90 mg) was followed by the same protocol as that of SF2 on ODS HPLC eluting with MeOH–H<sub>2</sub>O (80%) to obtain **4** (9.3 mg), **3** (5.4 mg), and **6** (5.2 mg). SF4 (49.2 mg) was separated on ODS HPLC with MeOH–H<sub>2</sub>O (82%) as a mobile phase to afford **7** (3.2 mg). Following by the same protocol, **1** (10.1 mg), **2** (3.8 mg), and **5** (4.6 mg) were obtained from SF5 (40.5 mg).

Lobophytone H (**1**): Amorphous powder; [ $\alpha$ ]<sub>D</sub><sup>25</sup> +93.1 (*c*=1.13, CHCl<sub>3</sub>); IR (KBr)  $\nu_{\max}$  3380, 2962, 2929, 1744, 1709, 1458, 1436, 1373, 1196, 1105 cm<sup>-1</sup>; <sup>1</sup>H- and <sup>13</sup>C-NMR data, see Tables 1 and 2; HR-ESI-MS *m/z* 705.4309 [M+Na]<sup>+</sup> (Calcd for C<sub>41</sub>H<sub>62</sub>O<sub>8</sub>Na, 705.4336).

Lobophytone I (**2**): Amorphous powder; [ $\alpha$ ]<sub>D</sub><sup>25</sup> +67.0 (*c*=0.27, CHCl<sub>3</sub>); IR (KBr)  $\nu_{\max}$  3444, 2958, 2928, 1709, 1459, 1375, 1205, 1081, 1062 cm<sup>-1</sup>; <sup>1</sup>H- and <sup>13</sup>C-NMR data, see Tables 1 and 2; HR-ESI-MS *m/z* 683.4621 [M+H]<sup>+</sup> (Calcd for C<sub>41</sub>H<sub>63</sub>O<sub>8</sub>, 683.4517).

Lobophytone J (**3**): Amorphous powder; [ $\alpha$ ]<sub>D</sub><sup>25</sup> -67.6 (*c*=0.40, CHCl<sub>3</sub>); IR (KBr)  $\nu_{\max}$  3560, 2957, 2931, 1740, 1712, 1459, 1375, 1249, 1070 cm<sup>-1</sup>; <sup>1</sup>H- and <sup>13</sup>C-NMR data, see Tables 1 and 2; HR-ESI-MS *m/z* 765.4540 [M+Na]<sup>+</sup> (Calcd for C<sub>43</sub>H<sub>66</sub>O<sub>10</sub>Na, 765.4548).

Lobophytone K (**4**): Amorphous powder; [ $\alpha$ ]<sub>D</sub><sup>25</sup> +68.6 (*c*=0.70, CHCl<sub>3</sub>); IR (KBr)  $\nu_{\max}$  3469, 2959, 2928, 1705, 1458, 1371, 1210, 1063 cm<sup>-1</sup>; <sup>1</sup>H- and <sup>13</sup>C-NMR data, see Tables 1 and 2; HR-ESI-MS *m/z* 723.4440 [M+Na]<sup>+</sup> (Calcd for C<sub>41</sub>H<sub>64</sub>O<sub>9</sub>Na, 723.4442).

Lobophytone L (**5**): Amorphous powder; [ $\alpha$ ]<sub>D</sub><sup>25</sup> +122.6 (*c*=0.19, CHCl<sub>3</sub>); IR (KBr)  $\nu_{\max}$  3435, 2959, 2929, 1739, 1706, 1458, 1374, 1207, 1060 cm<sup>-1</sup>; <sup>1</sup>H- and <sup>13</sup>C-NMR data, see Tables 1 and 2; HR-ESI-MS *m/z* 701.4604 [M+H]<sup>+</sup> (Calcd for C<sub>41</sub>H<sub>65</sub>O<sub>9</sub>, 701.4623), *m/z* 723.4425 (Calcd for C<sub>41</sub>H<sub>66</sub>O<sub>9</sub>Na, 723.4442).

Lobophytone M (**6**): Amorphous powder; [ $\alpha$ ]<sub>D</sub><sup>25</sup> +113.3 (*c*=0.38, CHCl<sub>3</sub>); IR (KBr)  $\nu_{\max}$  3466, 2959, 2927, 1724, 1706, 1459, 1375, 1207, 1059 cm<sup>-1</sup>; <sup>1</sup>H- and <sup>13</sup>C-NMR data, see Tables 1 and 2; HR-ESI-MS *m/z* 705.4327 [M+Na]<sup>+</sup> (Calcd for C<sub>41</sub>H<sub>62</sub>O<sub>8</sub>Na, 705.4337).

Lobophytone N (**7**): Amorphous powder; [ $\alpha$ ]<sub>D</sub><sup>25</sup> +137.5 (*c*=0.21, CHCl<sub>3</sub>); IR (KBr)  $\nu_{\max}$  3456, 2962, 2928, 1742, 1707, 1459, 1375, 1207, 1063 cm<sup>-1</sup>; <sup>1</sup>H- and <sup>13</sup>C-NMR data, see Tables 1 and 2; HR-ESI-MS *m/z* 751.4760 [M+Na]<sup>+</sup> (Calcd for C<sub>43</sub>H<sub>68</sub>O<sub>9</sub>Na, 751.4756).

**Assay for Inhibition of Lipopolysaccharide (LPS)-Induced Nitric Oxide (NO) Production and Cytotoxicity of Mouse Peritoneal Macrophage (PEMΦ)** Dexamethasone (DEX, positive control, 20 mm in dimethyl sulfoxide (DMSO)) and each compound (20 mm in DMSO) were diluted to 1–20 μM range at r.t. before experiment. The final percentage of DMSO in the reaction mixture was less than 0.5% (v/v). LPS (1 μg/ml), 4% sodium thioglycollate, RPMI1640, fetal bovine serum (FBS), phosphate buffered saline (PBS), 3-(4,5-dimethylthiazol-2-yl)-2,5-diphenyltetrazolium bromide (MTT) and Griess reagents were purchased from Sigma (St. Louis, MO, U.S.A.). Mouse peritoneal macrophages (PEMΦ) were obtained from C57BL6J male mice, and then plated onto 48 well plates and cultured for 2 h in Dulbecco's modified Eagle's medium (DMEM) containing 5% FBS at 5% CO<sub>2</sub> in 37 °C. Mouse PEMΦ were incubated with test compounds for 1 h at

37 °C before stimulation with 1 μg/ml of lipopolysaccharide (LPS) for 24 h. In primary test, blank control (enchylema) and LPS were added with compound (1 μM), and DEX (1 μM) was prepared. Cells (5 × 10<sup>5</sup> cells) were pre-incubated at 37 °C for 24 h in serum-free medium, and NO production was monitored by measuring nitrite levels in culture media using Griess reagent. Absorbance was measured at 548 nm in incubated media with Griess reagent for 10 min. Viable adherent cells were stained with MTT (2 μg/ml) for 4 h. Media was then removed and the formazan crystals produced were dissolved in DMSO (200 μl). Absorbance was tested at 540 nm. The cytotoxicity of PEMΦ was tested by MTT colorimetry.

One-way analysis of variance was applied for all statistical analyses by independent experiments. Individual values comparing by *t*-test and a *p*-value <0.01 were considered as significant.

**Antibiotic Assay** Antimicrobial and antifungal bioassays were conducted in triplicate by following the method in document<sup>19</sup> and the National Center for Clinical Laboratory Standards (NCCLS) recommendations.<sup>20</sup>

**Acknowledgments** This project was supported by grants from the National Hi-Tech Development Project (863 project) (No. 2010DFA31610, 2007AA09Z448, 2008AA09Z405), NSFC (No. 30930109), National Key Innovation Project (2009ZX09501-014, DYXM-115-02-2-09).

## References

- 1) Su J., Long K., Peng T., He C., Clardy J., *J. Am. Chem. Soc.*, **108**, 177–178 (1986).
- 2) Kusumi T., Igari M., Ishitsuka M. O., Ichikawa A., Itezono Y., Nakayama N., Kakisawa H., *J. Org. Chem.*, **55**, 6286–6289 (1990).
- 3) Leone P. A., Bowden B. F., Carroll A. R., Coll J. C., Meehan G. V., *J. Nat. Prod.*, **56**, 521–526 (1993).
- 4) Zeng L., Lan W., Su J., Zhang G., Feng X., Liang Y., Yang X., *J. Nat. Prod.*, **67**, 1915–1918 (2004).
- 5) Iwagawa T., Hashimoto K., Okamura H., Kurawaki J., Nakatani M., Hou D. X., Fujii M., Doe M., Morimoto Y., Takemura K., *J. Nat. Prod.*, **69**, 1130–1133 (2006).
- 6) Jia R., Guo Y., Chen P., Yang Y., Mollo E., Gavagnin M., Cimino G., *J. Nat. Prod.*, **70**, 1158–1166 (2007).
- 7) Bishara A., Rudi A., Benayahu Y., Kashman Y., *J. Nat. Prod.*, **70**, 1951–1954 (2007).
- 8) Iwagawa T., Hashimoto K., Yokogawa Y., Okamura H., Nakatani M., Doe M., Morimoto Y., Takemura K., *J. Nat. Prod.*, **72**, 946–949 (2009).
- 9) Yan P., Lv Y., Ofwegen L., Proksch P., Lin W., *Org. Lett.*, **12**, 2484–2487 (2010).
- 10) Lu Q., Faulkner D. J., *Nat. Prod. Lett.*, **10**, 231–237 (1997).
- 11) Tursch B., Hootele C., Kaisin M., Losman D., Karlsson R., *Steroids*, **27**, 137–142 (1976).
- 12) Babu U. V., Bhandari S. P. S., Garg H. S., *Indian J. Chem.*, **37B**, 576–578 (1998).
- 13) Edrada R. A., Peter P., Victor W., Ludger W., Leen O., *J. Nat. Prod.*, **61**, 358–361 (1998).
- 14) Anjaneyulu A. S. R., Venkateswar Rao G., Raju K. V. S., Murthy M. V. R. K., *Indian J. Chem.*, **34B**, 1074–1079 (1995).
- 15) Anjaneyulu V., Babu B. H., *Indian J. Chem.*, **32B**, 1198–1199 (1993).
- 16) Iguchi K., Kitade M., Yamada Y., Ichikawa A., Ohtani I., Kusumi T., Kakisawa H., *Chem. Lett.*, **2**, 319–322 (1991).
- 17) Yamada Y., Suzuki S., Iguchi K., Kikuchi H., Tsukitani Y., Horiai H., *Chem. Pharm. Bull.*, **28**, 2035–2038 (1980).
- 18) Jia R., Guo Y., Mollo E., Gavagnin M., Cimino G., *Helv. Chim. Acta*, **91**, 2069–2074 (2008).
- 19) Ding G., Li Y., Fu S., Liu S., Che Y., *J. Nat. Prod.*, **72**, 182–186 (2009).
- 20) Li E., Jiang L., Guo L., Zhang H., Che Y., *Bioorg. Med. Chem.*, **16**, 7894–7899 (2008).